Available online at www.sciencedirect.com

ScienceDirect

Polymer 49 (2008) 1037–1048

polymer

www.elsevier.com/locate/polymer

Electrically conductive in situ microfibrillar composite with a selective carbon black distribution: An unusual resistivity–temperature behavior upon cooling

Kun Dai, Zhong-Ming Li*, Xiang-Bin Xu

College of Polymer Science and Engineering, State Key Laboratory of Polymer Materials Engineering, Sichuan University, Chengdu, 610065 Sichuan, People's Republic of China

Received 28 July 2007; received in revised form 3 December 2007; accepted 23 December 2007
Available online 11 January 2008

Abstract

Carbon black (CB) filled electrically conductive in situ microfibrillar poly(ethylene terephthalate) (PET)/polyethylene (PE) composites (FCMC) with CB particles selectively localizing at the surfaces of PET microfibrils were successfully prepared through a slit die extrusion–hot stretch–quenching process. Resistivity–temperature behaviors of the FCMC samples were studied systematically during heating–cooling runs (HCR) with different top test temperatures. When the top test temperature was set as 140 °C, the resistivity abnormally increased during cooling below 100 °C, showing the cooling-induced resistivity increase. The room-temperature resistivity after one heating–cooling run was 4 orders of magnitude higher than that of the original samples. Thermal residual stresses developed in the interfaces between PET microfibrils and PE matrix were responsible for the cooling-induced resistivity increase, which led to the damage of the conductive network. The top test temperature dominated the cooling-induced resistivity increase of FCMC. There was a critical temperature, 150 °C, above which the cooling-induced resistivity increase disappeared. A model was proposed to illustrate this cooling-induced resistivity increase.

Keywords: Conductive polymer composite; In situ microfibrillar blend; Cooling-induced resistivity increase

1. Introduction

The positive temperature coefficient (PTC) effect and negative temperature coefficient (NTC) effect are the typical resistivity–temperature behaviors of carbon category materials (e.g., carbon black (CB) [1–9], carbon nanotubes [10–12]) filled conductive polymer composites (CPC), which are very often investigated because they are the basis of popular applications such as overcurrent, overtemperature protection devices, self-regulating heaters, etc. [13–16]. PTC and NTC are the sharp increase and the succeeding gradual decrease of the resistivity of CPC around the melting point of the matrix polymer, respectively. Up to now, to explain PTC mechanism, several theories have been proposed by Meyer [1,17], Ohe [18], and Voet [19], of which the thermal expansion theory is the universal viewpoint. For the NTC effect, it has been suggested that it is caused by the formation of a flocculated structure when the viscosity of the polymer is sufficiently low at elevated temperatures [20]. Nevertheless, the mechanisms about the resistivity–temperature behaviors are still incomplete [20,21]. One major reason is that too many parameters can affect PTC and NTC effects in very complex manners, including the features of the polymers, such as chemical structure, crystallinity; the properties of conductive fillers, such as the size of particles, aggregate shape; and the test conditions of PTC and NTC effects. Luo et al. found that crystallization process and crystallinity of the polymer matrix as well as its morphology have marked effects on PTC characteristics of a polyethylene (PE)/CB composite, and concluded that annealing is a good means of improving PTC intensity of the PE/CB composite [22]. Yi et al. considered that the mechanism for the

---

* Corresponding author. Fax: +86 28 8540 5324.
E-mail address: zm_li@263.net.cn (Z.-M. Li).

0032-3861/$ - see front matter © 2008 Elsevier Ltd. All rights reserved.
doi:10.1016/j.polymer.2007.12.043

PTC anomaly in semi-crystalline polymer composites is generally attributed to the relatively large change in specific volume of the polymer at its melting point [19,23]. Chan et al. studied the influence of the CB particle size on double PTC effects of CB/polypropylene (PP)/ultra-high molecular weight polyethylene (UHMWPE) composites [6], and suggested that a balance between the PTC intensity and the room-temperature resistivity can be achieved by using a mixture of large and small CB particles. Hirano et al. investigated the effect of heating rate on PTC behavior of SnO_2(Sb)-coated TiO_2/expoxy conductive thin films, and found that the larger heating rate can create a higher PTC intensity than the slower one [21].

The distribution of CB particles in the matrix also affects the PTC and NTC effects strongly. Narkis et al. found the distribution of CB on the interfaces of poly(4-methyl pentene-1) (TPX)/crosslinked ultra-high molecular weight polyethylene (XL-UHMWPE)/CB composites leads to a double PTC behaviors. The first PTC is attributed to the thermal expansion due to melting of the XL-UHMWPE phase, and the second PTC is related to the melting of the TPX matrix, affecting CB distribution in the blend [3]. Chan et al. observed that the CB/high density polyethylene (HDPE)/tetrafluoroethylene–ethylene (ETFE) composites also show a double PTC effect, and they supposed that the NTC effect in this system could not have been caused by the formation of flocculated structures, because the CB particles were selectively distributed in HDPE phases and the size of these phases was significantly large so that their mobility was extremely limited even at high temperatures [20].

However, to our knowledge, the majority of the works about resistivity–temperature behaviors of CPC are performed during heating process, such as the PTC and NTC effects mentioned above, the resistivity–temperature behavior during cooling process is almost neglected in the available literature [24]. Factually, the resistivity–temperature behavior in the cooling process is closely related to the behavior in the heating run, and vice versa. This deficiency may be one of the reasons that the mechanisms about the PTC and NTC effects have not been well established so far.

It is well known that a desired PTC performance requires a low room-temperature resistivity, a high PTC intensity, a low NTC intensity, a high electrical reproducibility, and a high PTC transition temperature, together with low conductive filler content [25]. During cooling, in one hand, the conductive network, which is generally regenerated during heating, will be destroyed partially because of the crystallization of the matrix from the melt [24], whereafter, with the shrinkage of composites and the increased concentration of conductive fillers in amorphous areas by the exclusion of polymer crystallites, the destroyed conductive network will be reconstructed and then leads to a decrease in resistivity. Until the temperature reaches the room temperature, then another room-temperature resistivity was obtained, and this resistivity is the initial point for next test or next application [24,26]. Therefore, the process will finally affect the room-temperature resistivity and the reproducibility of the CPC. On the other hand, the cooling process is related to the crystallization of the matrix polymer. The CPC with a high crystallinity matrix exhibits larger thermal expansion around the melting temperature than the CPC with a low one [23]. Larger thermal expansion shows a higher PTC intensity due to severe damage of the conductive network during heating. It is known that thermal treatment history affects the crystallinity of a semi-crystalline polymer. In the resistivity–temperature behavior tests, it affects the PTC effect further. Based on this, if several heating–cooling runs are performed, the thermal history will influence the crystallinity. The crystallization of the matrix polymer takes place during the cooling process, thus influencing the PTC intensity and the reproducibility. Therefore, the studies on the resistivity–temperature behaviors during the cooling process are of high importance.

In our previous work [4,27–29], the concept of in situ microfibrillar blend has been utilized to fabricate a new conductive polymer composite with a conductive microfibrillar network in which the CB particles are predominately localized in poly(ethylene terephthalate) (PET), the PE was used as matrix. The CPC with such architecture shows a low percolation threshold (5.0 vol%) and strong PTC effect. Anomalously, the PTC intensity of the CPC decreases gradually with the increasing time of isothermal treatment above the melting point of the polymer matrix [4]. The inhomogeneous surface microstructure and the large size of the microfibrils are the key factors controlling this PTC attenuation. Based on these results, another electrically conductive in situ microfibrillar composite with a selective CB distribution has been prepared, in which the CB particles assume a gradient distribution in the outer layer of the in situ PET microfibrils. Due to the more perfect conductive network, a low percolation threshold of 3.8 vol% has been achieved [30].

The present work studied the resistivity–temperature behaviors of the CB filled electrically conductive in situ microfibrillar PET/PE composites (FCMC) with CB particles selectively localizing at the surfaces of PET microfibrils. The PTC and NTC effects of the FCMC were measured during heating–cooling runs (HCR) with different top test temperatures. The resistivity–temperature behavior during cooling was particularly concerned.

2. Experimental

2.1. Materials

The main materials used in this work include electrically conductive CB, high density PE and PET. The CB, model VXC-605, from Cabot Co. Ltd., with a dibutyl phthalate (DBP) absorption value of $148 \pm 15\ cm^3/100\ g$, was dried at 120 °C for 10 h to get rid of the water before use. PE (model 5000S) is a commercial high density PE of DaQing Petroleum Chemical Co., Daqing, China, and its melt flow rate is 0.9 g/10 min at 190 °C, exerting a load of 21.6 N. PET was friendly donated by LuoYang Petroleum Chemical Co., LuoYang, China, which is a commercial grade of textile polyester with a number average molecular weight of ca. 2.3×10^4 g/mol.

2.2. Preparation of CB filled electrically conductive in situ microfibrillar PET/PE composites

PET was dried in a vacuum oven at 100 °C for at least 12 h prior to processing. The FCMC was obtained with the following three steps. First, PE was fed into an internal mixer and held for 5 min at 180 °C, and then CB particles were added and melt was mixed at the same temperature for 5 min. The CB/PE masterbatch was granulated and drily mixed with PET chips. Secondly, the mixture obtained was extruded through a slit die in a single-screw extruder. The temperature profile was 190 °C, 250 °C, 275 °C and 270 °C, from the hopper to the exit, respectively. The extrudate was hot stretched at a line speed of ca. 1.1 m/min by a take-up device with two pinching rolls to form the microfibrils [27–30]. After hot stretching, the extrudate was immediately quenched in a cold water (20 °C) bath to preserve the microfibrils in the composite. The ribbon with a thickness of about 0.2 mm was thus obtained. Subsequently, the ribbon was pelletized, and then compression molded into $10 \times 10 \times 2\ \text{mm}^3$ board at 150 °C (the processing temperature of PE) for 10 min with a pressure of ca. 10 MPa. All these sheets were cooled to room temperature by cold compression molding for 5 min. Due to the high melting point of PET (about 257 °C [4]), the in situ PET microfibrils can be successfully reserved in the composite during molding.

2.3. Morphological observation

The specimens were frozen in liquid nitrogen for 1 h, then quickly impact fractured. The fracture surfaces were covered with a layer of gold to make them conductive, and then observed with a JEOL JSM-5900LV scanning electron microscope (SEM). In order to clearly examine the morphology of the dispersed phase, some specimens were immersed in hot xylene at about 125 °C for 15 h to dissolve the PE matrix away.

2.4. Electrical properties and resistivity–temperature behaviors test

Before the electrical properties and resistivity–temperature behaviors test, all the samples were annealed for 8 h at 80 °C to remove the effect of internal stress developed during the processing history (mainly the compression molding). When the volume resistivity of samples is below $10^6\ \Omega\,\text{cm}$, the volume electrical resistivity was measured by a four-probe method (ASTM D-991) using two multimeters and a voltage supply. The four-probe method can effectively avoid the contact resistance which affects the precision of the measurement. When the volume resistivity is relatively low, this method has adequate preciseness. A high resistivity meter was used when the volume resistivity of the samples is beyond $10^6\ \Omega\,\text{cm}$. The sample dimensions for low and high resistivity measurements were $2 \times 10 \times 100\ \text{mm}^3$ and $2 \times 100 \times 100\ \text{mm}^3$, respectively.

In resistivity–temperature test, the sample ($2 \times 10 \times 100\ \text{mm}^3$), which was immersed in silicone oil of a temperature-controlled apparatus to avoid oxidation, was heated from room temperature to different top test temperatures (140 °C, 150 °C, 180 °C) at 2 °C/min and held at this temperature for a predetermined time (3 min), then cooled to 25 °C at the same rate. The data were recorded by a computer. For the sake of exploring the influence of the thermal treatment, some samples were annealed at 140 °C or 180 °C for several hours (1 h and 10 h), and then the heating–cooling test was also applied as above. Several samples were measured at 0.5 °C/min in the cooling process to examine the effect of cooling rate on the resistivity–temperature behavior.

In practice, the sample can hold its initial shape during the resistivity–temperature test because the PET microfibrils form a network in the composite, and remain solid all the time, even at 180 °C, which is still far below the melting point of PET (about 257 °C).

2.5. Thermal property test

Thermal analyses were carried out by a Netzsch DSC 204 differential scanning calorimeter. The samples were heated to 140 °C at 2 °C/min, kept for 3 min, and then cooled at 2 °C/min to room temperature, a heating–cooling journey similar with resistivity–temperature tests. The heat capacity versus temperature was recorded for each scan.

For the sake of brevity, in the resistivity–temperature tests, the heating–cooling run of the top test temperature 140 °C, 150 °C and 180 °C are referred to HCR140, HCR150 and HCR180, respectively.

3. Results

3.1. Morphology and electrically conductive properties

In order to thoroughly understand the resistivity–temperature behaviors of FCMC, it is necessary to resurvey the typical morphology and the percolation behavior of the microfibrillar composites, as shown in Figs. 1–3.

Fig. 1(a) indicates that the well-defined PET microfibrils were generated in situ in the composite (3.5 vol% CB). The microfibrils' diameter is about 1–5 μm, while their length is hard to estimate due to the limited observed region. Fig. 1(b) shows the typical morphology of FCMC fractured perpendicular to the stretch direction. Numerous CB particles accumulated in the surfaces of the PET microfibrils. In contrast, there are nearly no CB particles in the center of the PET microfibrils. This unique structure is in favor of the transfer of electrons between neighboring microfibrils, and thus the conductivity will undoubtedly be enhanced. Fig. 2(a) shows the morphology of the specimens with a higher CB concentration of 4.93 vol%, in which fine microfibrils can also be observed obviously. Fig. 2(b) displays the morphology of FCMC fractured perpendicular to the stretch direction. Besides the regions around the microfibrils, CB particles, basically in the form of aggregates, appear in the matrix. It indicates that when the surface of the microfibrils was completely covered with CB particles, the CB particles encountered

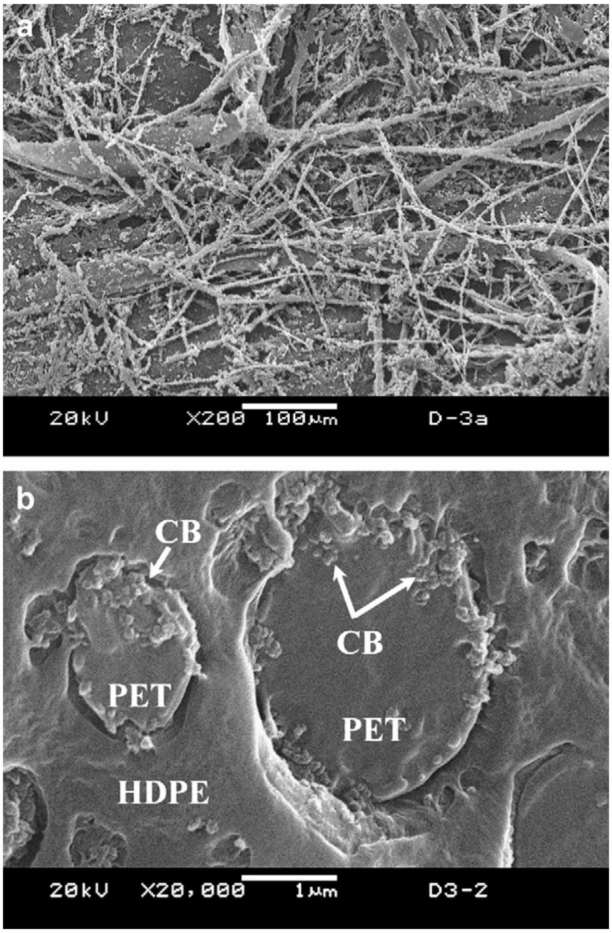

Fig. 1. SEM micrographs of the CB filled electrically conductive in situ microfibrillar PET/PE composite with selectively locating CB in the surfaces of the PET microfibrils. In (a), the PE matrix was etched away by hot xylene for clear observation; (b) is The SEM micrograph of the cryofractured surface. The volume ratio of PET and PE is 1:3.2, and the CB loading is 3.5 vol%.

hindrance in migration to PET phase, and some of them have to stay in the matrix. These CB particles were almost in the form of aggregates. Nevertheless, the CB aggregates in the matrix can also help to build electrical networks together with the CB coated microfibrils. Detailed description about the morphology development and the construction of the conductive network of FCMC has been reported elsewhere [30].

Fig. 3 displays the correlation between the volume resistivity and CB loading for FCMC. The percolation threshold is estimated from Fig. 3, which is as low as ca. 3.8 vol%. At the CB percolation level, the resistivity of the microfibrillar composite is decreased by about 12 orders of magnitude. In the present work, the FCMC with 4.93 vol% CB was used to study the resistivity–temperature behaviors. This CB content is just beyond the percolation threshold, the conductive network constructed by CB particles coated PET microfibrils is just formed and thus sensitive to the temperature field [31].

3.2. Thermal properties

The thermal expansion of CPC, which has been demonstrated to be able to destroy the conductive network of the CPC in the

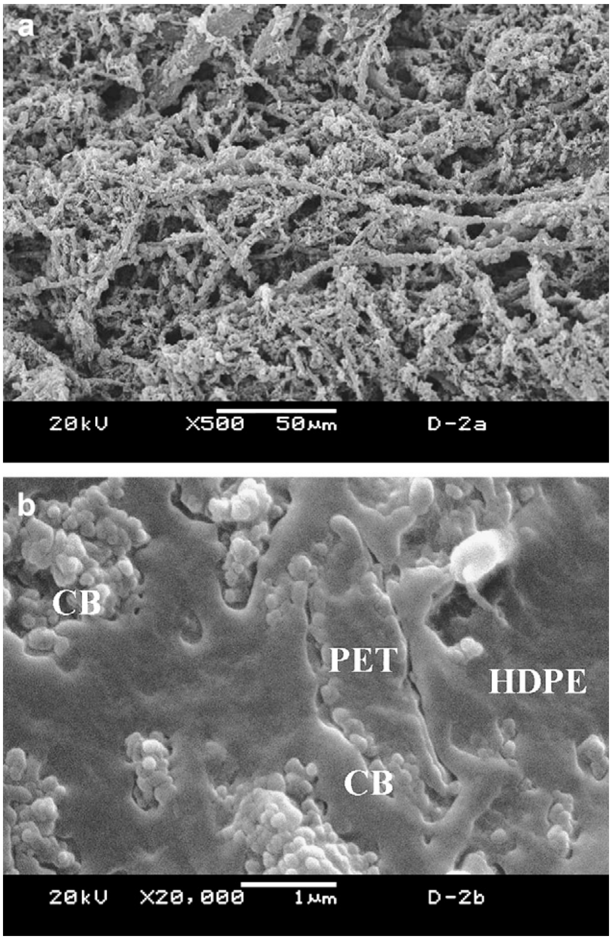

Fig. 2. SEM micrographs of the CB filled electrically conductive in situ microfibrillar PET/PE composite with selectively locating CB in the surfaces of the PET microfibrils. In (a), the PE matrix was etched away by hot xylene for clear observation; (b) is The SEM micrograph of the cryofractured surface. The volume ratio of PET and PE is 1:3.2, and the CB loading is 4.9 vol%.

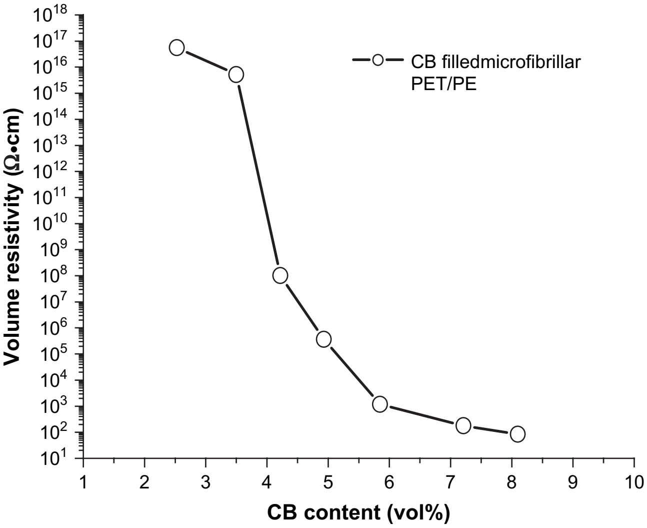

Fig. 3. Volume resistivity versus CB content of CB filled electrically conductive in situ microfibrillar PET/PE composites. The volume ratio of PET and PE is 1:3.2.

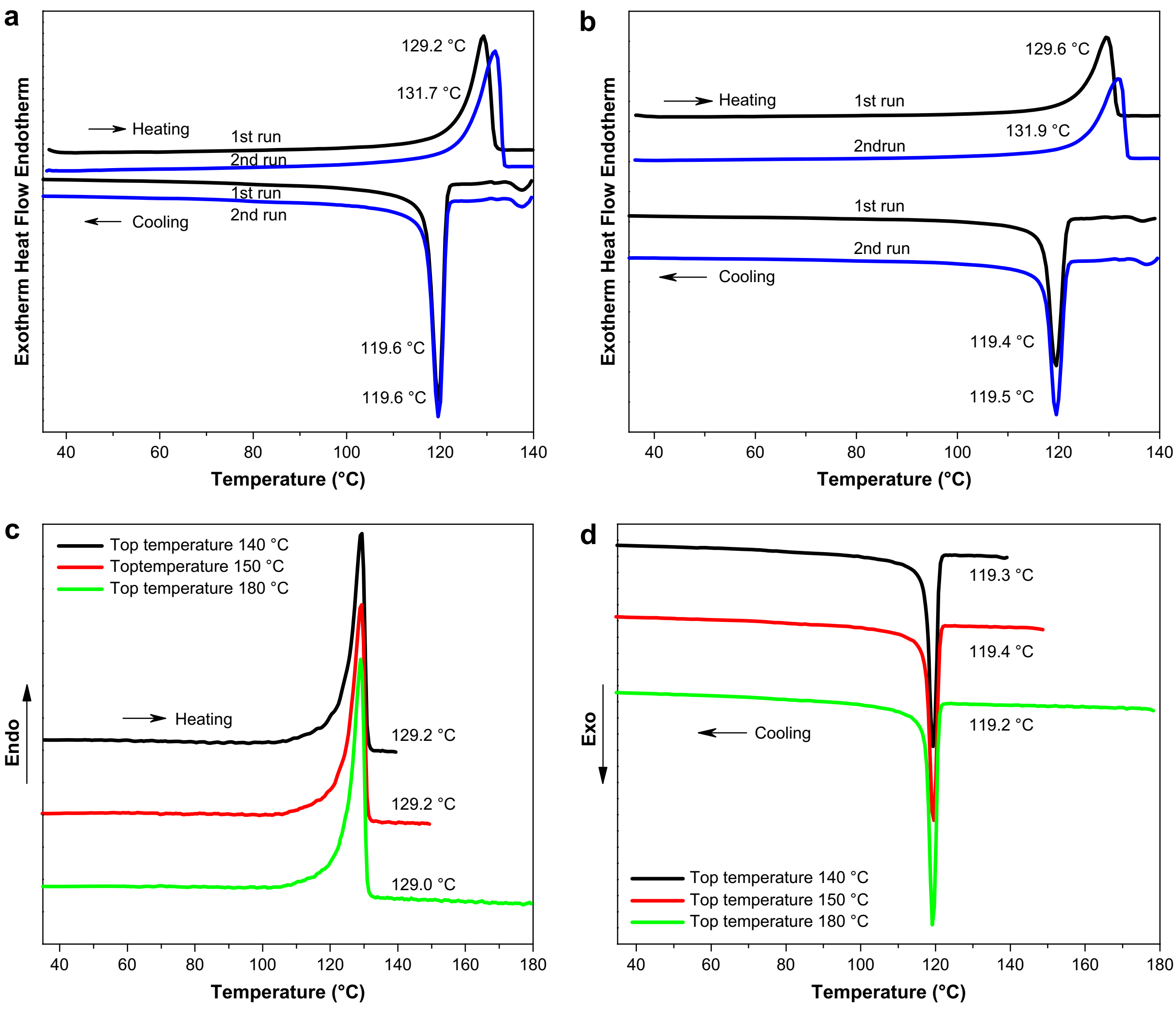

Fig. 4. DSC curves of the CB filled electrically conductive in situ microfibrillar PET/PE composite with 4.93 vol% CB (a) and the common CB/PE composite with 8.68 vol% CB (b) in the heating and cooling processes, respectively; (c) and (d) are the traces of melting and cooling behaviors of CB filled electrically conductive in situ microfibrillar PET/PE composite from 35 °C to 140 °C, 150 °C and 180 °C, respectively. The heating and cooling rates are both 2 °C/min.

heating process, is the universal theory to elucidate the PTC effect, because the sharp increase of the volume expansion and the PTC effect always simultaneously occur around the melting temperature of the semi-crystalline polymer matrix. In the present work, the temperature range of resistivity–temperature test exceeds the melting temperature of PE, but far below the melting point of PET (257 °C). During test, PE undergoes melting/crystallization transition leading to a large thermal expansion/contraction, but PET has only common linear expansion/contraction. Although cold crystallization of PET is common in many cases, in our experiment, after the manufacturing processes, especially after 8 h isothermal treatment, the cold crystallization of PET is not obvious. Actually, the cold crystallization peak of PET is indeed not observed in the DSC curves (see Fig. 4). Hence, the thermal behavior of PE matrix is a key element affecting the resistivity–temperature behaviors. Accordingly, the thermal analyses of the FCMC and CB/PE composites was conducted by DSC from 25 °C to 140 °C at 2 °C/min to match the resistivity–temperature test of HCR140.

Fig. 4(a) shows the DSC scans of the FCMC for two heating–cooling runs. In the first run, the melting point of PE matrix appears at 129.25 °C, and the maximum crystallization temperature is 119.60 °C. In the second run, the melting point rises to 131.73 °C from 129.25 °C, because PE has formed more perfect crystals after the thermal treatment in the first run. The maximum crystallization temperature of PE is nearly the same for two runs (ca. 119.63 °C). The DSC curves of the CB/PE composite (Fig. 4(b)) are similar to those of the FCMC, but the melting point of PE is a little higher than that of PE in the FCMC. DSC traces of the melting and cooling behaviors of FCMC up to 140 °C, 150 °C and 180 °C are shown in Fig. 4(c) and (d). Detailed information of DSC traces up to different top test temperatures is listed in Table 1 (melting enthalpy of polyethylene crystal with 100% crystallinity

Table 1
Detailed information of DSC traces up to different top test temperatures: 140 °C, 150 °C and 180 °C

T_p (°C)	$T_{c\text{-onset}}$ (°C)	T_c (°C)	ΔH_c (J/g)	T_m (°C)	$T_{m\text{-end}}$ (°C)	X_c (%)
140	121.0	119.3	134.4	129.2	130.8	48.6
150	121.1	119.4	132.9	129.2	130.8	49.3
180	120.9	119.2	137.4	129.0	130.7	50.2

T_p, the top test temperature; $T_{c\text{-onset}}$, onset temperature on DSC exotherm; T_c, maximum crystallization temperature; ΔH_c, enthalpy of crystallization; T_m, melting temperature; $T_{m\text{-end}}$, the end of the melting temperature; X_c, the crystallinity.

was set as 293 J/g in this study [32]). Apparently, the shapes and the peak values of these curves appear to be almost the same.

3.3. Resistivity–temperature behaviors

In most studies on the resistivity–temperature behaviors of PE based CPC, surprisingly, the top test temperature is always fixed at only one temperature, and it is much higher than the melting point of PE (always about 130 °C) [3,31,33]. In fact, different top test temperatures give rise to different thermal treatment histories, consequently, leading to various conductive networks which undoubtedly affect the overall resistivity–temperature behaviors.

If the top test temperature is fixed at a temperature near the melting point of the matrix, e.g., 140 °C, the CPC has a very high viscosity throughout the measurement, which can restrict the thermal motion of the conductive components. In this case, what happens for the resistivity–temperature behavior of CPC? This has not been concerned in the available literature. For the applications of CPC, taking overcurrent as an example, the composite has an absolute possibility to experience such a temperature just above the melting point. In the present work, the resistivity–temperature behaviors are first studied using the top test temperature of 140 °C, i.e., HCR140.

As shown in Fig. 5, during heating, the resistivity of the composite increases with temperature, the PTC effect appears at the temperature around the melting point, ca. 130 °C, of PE, where the resistivity has a sharp increase for more than 4 orders of magnitude. The universal thermal expansion theory mentioned above can explain this PTC effect. Around the melting temperature of PE, the melting of the crystalline region in PE results in a dramatic increase in the volume of the composite. Consequently, the thermal expansion causes severe separation of the previously contacted conductive PET microfibrils, and thus the conductive network in the composite becomes defective, leading to a sharp increase in the resistivity.

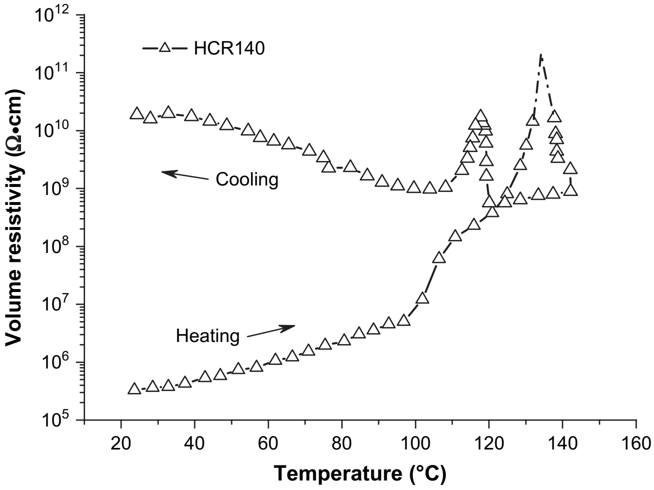

Fig. 5. Resistivity–temperature relationship of the CB filled electrically conductive in situ microfibrillar PET/PE composite in the heating–cooling run with a top test temperature of 140 °C (HCR140). The imaginary line denotes that the resistivity is beyond the test specification of the electrical meter. The heating and cooling rates are both 2 °C/min.

After the PTC effect region, the resistivity of the CPC decreases with further increasing temperature, exhibiting the so-called NTC effect. It is generally believed that the NTC effect is related to the agglomeration of filler particles in the molten matrix [34–36]. For the FCMC, the agglomeration of CB coated PET microfibrils forms gradually and thus leads to the contact of the conductive microfibrils to produce new conductive paths [4]. The amount of the conductive paths enlarges with increasing temperature, and consequently the NTC effect occurs.

During cooling, initially, the resistivity almost remains invariable with decreasing temperature. When the temperature reduces to the crystallization temperature of PE, due to the presence of PE crystallites, the conductive network in the molten matrix is broken and thus deteriorates the conductivity of the composite. Subsequently, both crystallization shrinkage and linear thermal shrinkage due to the decreasing temperature produce more conductive contact and thus result in fine conductivity [24], leaving a resistivity peak around the maximum crystallization temperature of PE.

When the temperature reduces below the maximum crystallization temperature of PE (ca. 119.6 °C), surprisingly, the resistivity of the composite does not reduce any longer; on the contrary, it substantially increases during cooling, exhibiting cooling-induced resistivity increase, which is the opposite to the conventional rule. At the end of the heating–cooling run, the room-temperature resistivity of the FCMC becomes 4 orders of magnitude higher than the initial room-temperature resistivity. In other words, after a heating–cooling run, quite unlike the general case [37,38], in which the conductivity of a CPC is enhanced or a little reduced, the conductivity of the FCMC is seriously deteriorated. To our knowledge, the cooling-induced resistivity increase has not been reported in the literature.

To probe the reproducibility of this anomalous resistivity–temperature phenomenon, some samples were tested for two heating–cooling cycles (HCR140). To describe the results more clearly, we changed the temperature of the horizontal axis to the time. Fig. 6(a) and (b) display the resistivity–temperature behaviors of the FCMC samples for the 1st and 2nd run, respectively. The 1st run is nearly the same as Fig. 5. For the 2nd run, during heating, the resistivity shows a little increase, whereafter, in the proximity of the melting point of PE matrix, the PTC effect also happens. In the cooling process below 100 °C, the resistivity also shows a gradual increase, which indicates the satisfactory repeatability of the cooling-

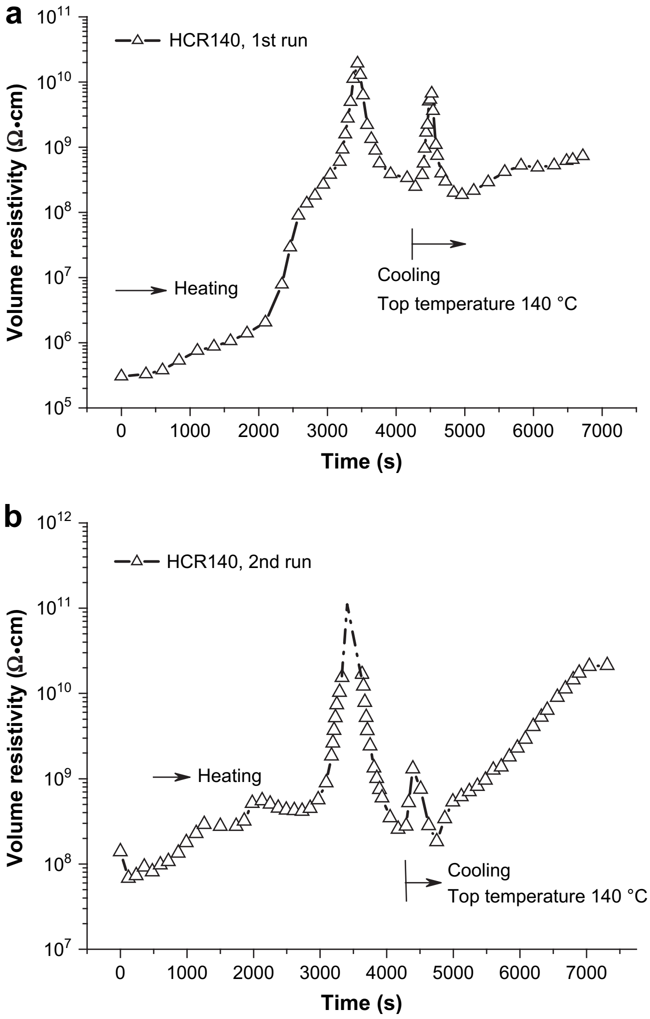

Fig. 6. Resistivity–temperature relationship of the CB filled electrically conductive in situ microfibrillar PET/PE composite in the heating–cooling run with a top test temperature of 140 °C (HCR140). In order to describe the results obtained more clearly, the temperature of the horizontal axis was changed with time; (a) and (b) are the first and the second run, respectively. The imaginary line denotes that the resistivity is beyond the test specification of the electrical meter. The heating and cooling rates are both 2 °C/min.

induced resistivity increase. Because the final resistivity after the 2nd run is beyond the limit of the test specification of the high resistance meter, more heating–cooling runs cannot be attainable.

For comparison, the resistivity–temperature behavior was probed through elevating the top test temperature from 140 °C to 180 °C (i.e., HCR180), a higher top test temperature frequently employed in many studies [3,33]. Fig. 7 shows the resistivity–temperature behaviors of FCMC sample in HCR180. During heating, the PTC and NTC effects behave like those in HCR140. However, during cooling below 100 °C, unlike the HCR140, the resistivity does not rise any longer, but decreases like the conventional case. After the heating–cooling run, the room-temperature resistivity of the composite is much lower than that of the original sample (from 2.3×10^{5} Ω cm to 8.4×10^{4} Ω cm), indicating a very fine conductive network generated through reorganization of the conductive PET microfibrils, which is consistent with the conventional cases reported in the literature [37] and our previous works [4].

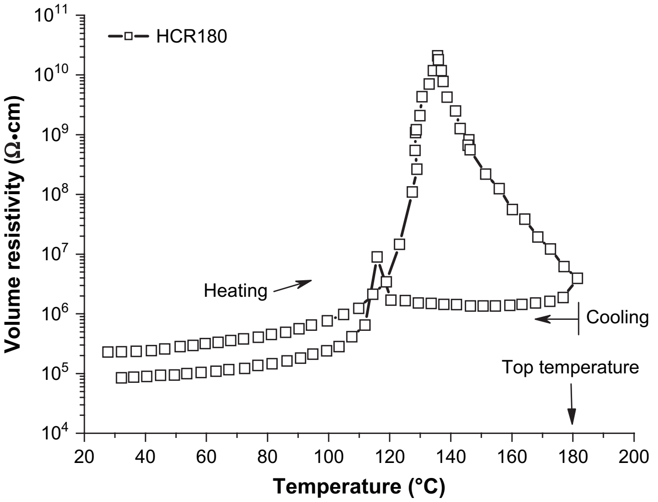

Fig. 7. Resistivity–temperature relationship of the CB filled electrically conductive in situ microfibrillar PET/PE composite in the heating–cooling run with a top test temperature of 180 °C (HCR180). The heating and cooling rates are both 2 °C/min.

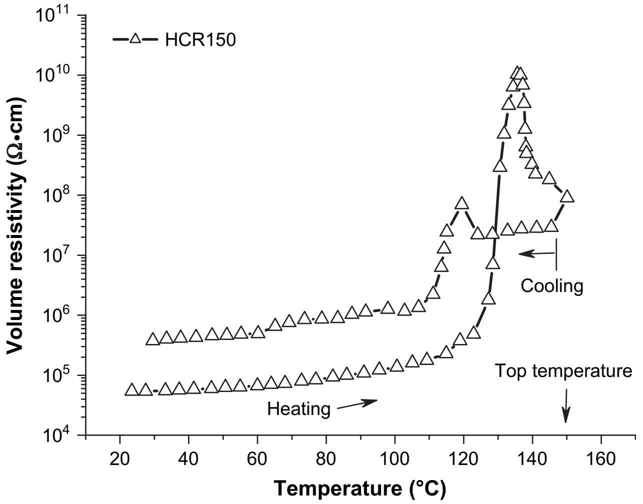

Fig. 8. Resistivity–temperature relationship of the CB filled electrically conductive in situ microfibrillar PET/PE composite in the heating–cooling run with a top test temperature of 150 °C (HCR150). The heating and cooling rates are both 2 °C/min.

When the top test temperature was set at 150 °C (HCR150), a temperature between 140 °C and 180 °C, the resistivity–temperature behavior is shown in Fig. 8. It is found that, in the cooling process below 100 °C, the resistivity does not rise but reduces with the temperature weakly. Nevertheless, the room-temperature resistivity of the sample is slightly higher than the original sample.

The above results indicate the top test temperature dominates the cooling-induced resistivity increase. There is a critical temperature around 150 °C, at which the room-temperature resistivity after heating–cooling runs almost equals the original resistivity. Too high top test temperature eliminates the

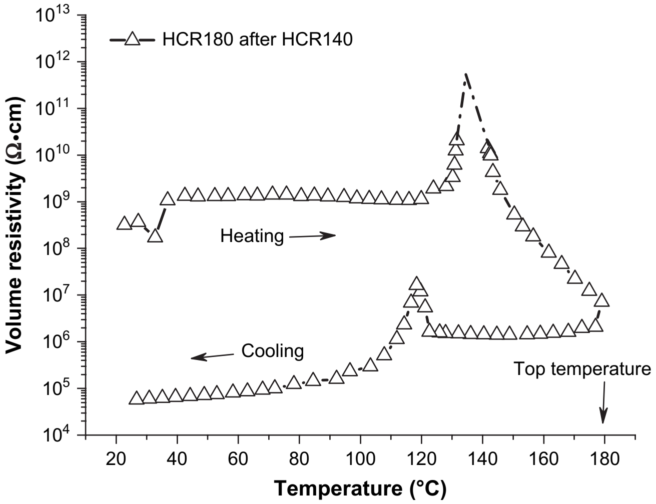

Fig. 9. Resistivity–temperature relationship of the CB filled electrically conductive in situ microfibrillar PET/PE composite in the heating–cooling run with a top test temperature of 180 °C (HCR180) after a heating–cooling run with a top test temperature of 140 °C (HCR140). The heating and cooling rates are both 2 °C/min. The imaginary line denotes that the resistivity is beyond the test specification of the electrical meter.

cooling-induced resistivity increase. The subsequent question is whether there is still the cooling-induced resistivity increase for the samples which have undergone a heating–cooling run. To answer this question, two measurements were performed: the resistivity–temperature relationship tests for the samples during HCR180 after a HCR140, and for the samples during HCR140 after a HCR180. Fig. 9 shows the resistivity–temperature behaviors of HCR180 after a HCR140. It is found that the room-temperature resistivity of the sample reduces for about 3 orders of magnitude throughout the HCR180. That is, the cooling-induced resistivity increase does not appear any longer. Fig. 10 shows the resistivity–temperature behaviors of HCR140 after a HCR180. Apparently, the cooling-induced resistivity increase does not yet exist.

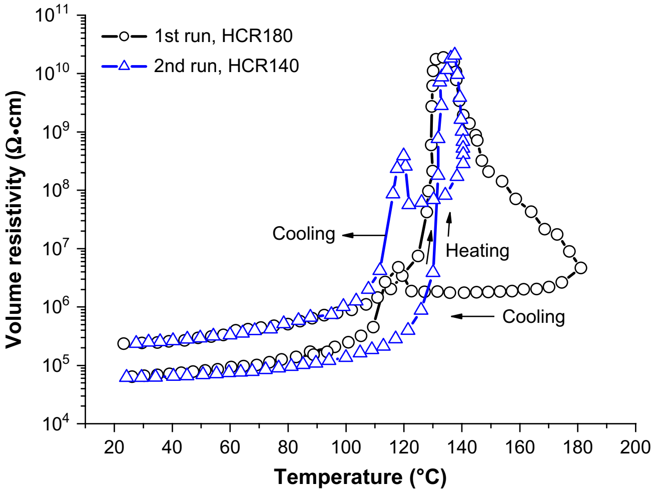

Fig. 10. Resistivity–temperature relationship of the CB filled electrically conductive in situ microfibrillar PET/PE composite in the heating–cooling run with a top test temperature of 140 °C (HCR140) after a heating–cooling run with a top test temperature of 180 °C (HCR180). The heating and cooling rates are both 2 °C/min.

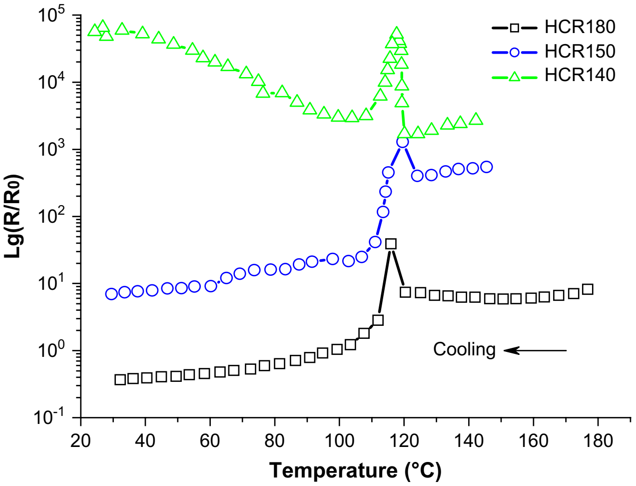

Fig. 11. Resistivity–temperature relationship of the CB filled electrically conductive in situ microfibrillar PET/PE composite during cooling. The top test temperatures of samples are 140 °C, 150 °C and 180 °C, respectively. The rates are all 2 °C/min. R is the resistivity during cooling. R_0 is the room-temperature resistivity of the original samples. The heating and cooling rates are both 2 °C/min.

For comparison, the resistivity–temperature behavior during cooling of the FCMC samples after different top test temperatures is summarized in Fig. 11. To understand the curves better, the vertical axis is changed to the ratio of the resistivity in the cooling process (R) to the room-temperature resistivity of the original samples (R_0), which is defined as the relative resistivity. Quite clearly, the resistivity–temperature behavior of the samples below 100 °C has a strong dependence of the top test temperature of the heating–cooling runs. The resistivity of the samples with decreasing temperature below 100 °C for HCR140, HCR150 and HCR180 show ascending and descending tendency, respectively. The sample with the lowest top test temperature (140 °C) shows the highest relative room-temperature resistivity and the sample with the highest top test temperature 180 °C displays the lowest relative room-temperature resistivity.

Though the thermal movement of the CB coated PET microfibrils is very slow due to the microfibrils' large size, it indeed exists, especially in the melt, and depends on the residence time. That is, the residence time of the microfibrils above the melting temperature of PE definitely affects the resistivity–temperature behavior of the sample. To intensify the influence of the residence time, the sample was isothermally treated at 180 °C for 10 h, and then, a HCR180 was applied to study its resistivity–temperature behavior, as shown in Fig. 12. Compared with the sample without thermal treatment shown in Fig. 7, the PTC intensity decreases obviously (only 1.2, the sample without thermal treatment is nearly 5 under the same condition. The PTC intensity is defined as $\log R_m/R_{25}$, R_m is the maximum resistivity during heating, R_{25} is the resistivity at 25 °C), and the NTC effect nearly disappeared. This indicates that the perfect conductive network was formed by fine contact of CB coated PET microfibrils during the long

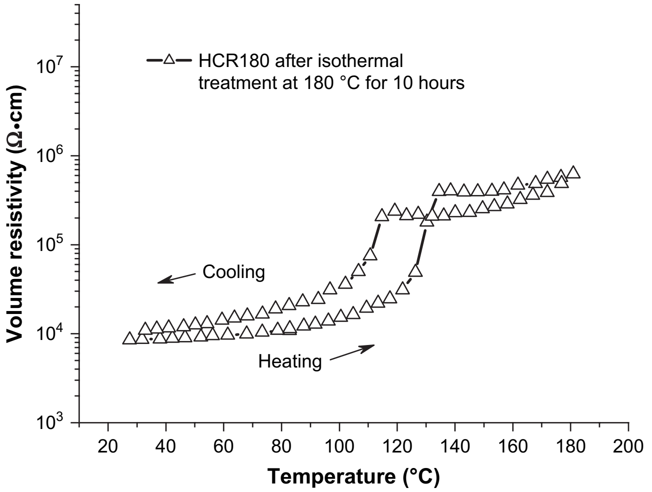

Fig. 12. Resistivity–temperature relationship of the CB filled electrically conductive in situ microfibrillar PET/PE composite in the heating–cooling run with a top test temperature of 180 °C (HCR180) after 10 h isothermal treatment. The heating and cooling rates are both 2 °C/min.

time isothermal treatment. The separate CB particles (possibly agglomerates) in the PE matrix would also help to construct a fine conductive network. This case also indicates that a long term thermal treatment brings out gradual aggregation of conductive components of FCMC, and ultimately, generates a fine conductive network.

4. Discussion

Why did this cooling-induced resistivity increase of the FCMC for HCR140 generate during cooling? The origin is discussed as follows.

It has been well established that the conductive network in the CPC can reorganize during heating and cooling, which influences the overall resistivity–temperature behavior of the CPC. Furthermore, the conductive structure generated during heating has an effect on the electrical properties of the succeeding cooling. Upon heating, the volume of the FCMC samples increase sharply due to the melting of PE crystallites, so the conductive network is broken down dramatically. The amount of conductive paths reduces and many conductive contacting points of the microfibrils are separated. As the temperature rises up to 140 °C, the sample of HCR140 enters the cooling process, while the sample for HCR180 still experiences the treatment from 140 °C to 180 °C, and then to 140 °C. There is an additional high temperature treatment time for 40 min (2 °C/min for both heating and cooling) for HCR180 sample, and the separated PET microfibrils have more time and energy to aggregate to form a fine conductive network. But for HCR140 sample, the separated PET microfibrils have not enough time and energy to generate a fine network, so it goes into the cooling process with a poor conductive network. The condition of the conductive network is the basic parameter influencing the resistivity–temperature behaviors of FCMC during cooling.

The top test temperature 140 °C is below the equilibrium melting temperature of PE, and at the beginning of cooling, an earlier crystallization and smaller spherulites may occur because of the self-seeding. The DSC results from Table 1 show that the onset crystallization temperatures for HCR140, HCR150 and HCR180 are nearly the same, hence the influence of earlier crystallization is very weak. Usually, if the temperature is relatively low, semi-crystalline polymer crystals do not melt completely, so some tiny crystallites still survive in the melt. Once the melt is cooled, these crystallites can act as nucleating sites, thus leading to more small crystals. In the present work, the DSC results show the melting temperature and melting end temperature of PE matrix are about 129.3 °C and 130.8 °C, respectively (see Table 1). For the HCR140 (with a heating rate of 2 °C/min), PE has stayed for a rather long time (about 12.5 min, 9.5 min plus the additional residence time of 3 min at 140 °C) above the melting temperature, so it is believed that the amount of the crystallites surviving in the PE melt is very small, and have little influence on the conductivity behavior during cooling. On the other hand, the conductive component (CB coated microfibrils) has large size. The small variation of crystallite size has, therefore, a very weak influence on the conductivity of the composite. Below 100 °C, one of the important factors affecting the resistivity–temperature behaviors of FCMC is the thermal residual stress.

For a two-phase or multi-phase polymer system, because of the difference of the thermal expansion coefficient between different components, with the change of temperature, thermal residual stress develops in the interface. Boyce et al. proposed an equation to calculate the thermal residual stress occurring in the matrix and homogenized particle due to a temperature change ΔT as follows [39]:

$$\sigma = \frac{K_{\mathrm{p}}\left(\gamma_{\mathrm{m}} - \gamma_{\mathrm{p}}\right)\Delta T}{1 + \frac{1}{1-c}\frac{K_{\mathrm{p}}}{K_{\mathrm{m}}}\left[\frac{1+\nu_{\mathrm{m}}}{2(1-2\nu_{\mathrm{m}})} + c\right]} \tag{1}$$

where σ is the thermal stress, K is the bulk modulus, γ is the volumetric coefficient of thermal expansion, ν is the Poisson's ratio. The subscripts p and t denote particles and matrix, respectively. Taking polybutadiene (PB)/polystyrene (PS) blend as an example, according to Eq. (1), the thermal stress is 8.64 MPa assuming PB particles in an infinite matrix, which is at least 10% lower than 9.68 MPa from the concentric shell PB/PS (the temperature from 25 °C down to −160 °C) [39]. Sue et al. used Eq. (2) to estimate the thermal residual stresses in the interface of the polycarbonate (PC)/PE blend ($\gamma_{\mathrm{m}} = 2 \times 10^{-4}\ \mathrm{K}^{-1}$, $\gamma_{\mathrm{p}} = 2 \times 10^{-4}\ \mathrm{K}^{-1}$, $\Delta T = -185\ °\mathrm{C}$, PE/PC = 3.3 wt%) [40], and found that, in contrast to the general speculation, the thermal stress between the PE and PC was surprisingly strong (as high as 30 MPa).

The thermal expansion coefficients of PET and PE are $2.5 \times 10^{-5}\ \mathrm{K}^{-1}$ and $1.6 \times 10^{-4}\ \mathrm{K}^{-1}$, respectively, showing a large difference. As a sort of rigid filler, CB has a much smaller thermal expansion coefficient than the two polymers PE and PET. Unfortunately, because the length of the PET microfibrils is not uniform and also hard to measure, and the shape of CB particles is also very complex, it is almost impossible to estimate the thermal residual stresses of FCMC in terms of Eq. (1). Nevertheless, due to the large length/diameter ratio of PET microfibrils and the complex distribution of CB particles, it can be understood that a large thermal residual stresses must exist at the interfaces between PET and PE, so does the interfaces between CB and the polymer PE or PET.

Upon cooling below 100 °C in HCR140, the crystallization of PE has been completed; there are two major factors controlling the resistivity–temperature behavior, including the thermal residual stresses mentioned above and the shrinkage of polymer components (especially the shrinkage of PE matrix). These two factors have opposite effects on the formation of the conductive network. The thermal residual stresses lead to irregular motion of the PET microfibrils and much breakage of conductive contact, so the conductive network will be broke partly and it results in the poor conductivity of FCMC; shrinkage of polymers enhances the contact of PET microfibrils and leads to fine conductivity.

For the sample during HCR140, firstly, as described above, a fine contact does not form in the heating process due to limited thermal treatment time. So at the beginning of the cooling process, because the aggregation of PET microfibrils is not enough, the conductive network, i.e., the contact situation between different PET microfibrils, is poor. The distances between PET microfibrils of the samples of HCR140 are also larger than the samples of HCR180 during cooling. The conductive paths of HCR140 are vulnerable. Secondly, because of the absent adhesion between PET and PE, voids exist at the interface (Figs. 1 and 2) and thus the conductive contact of CB coated PET microfibrils is further poor. Finally, the distribution of both PET microfibrils and CB particles are nonhomogeneous, which can also result in the internal stress and bad contact of PET microfibrils. All these factors indicate that, during cooling, the fragile conductive contact of the FCMC samples can be destroyed easily by the thermal residual stresses. According to the above discussion that the distances between PET microfibrils are large for HCR140, so the action of the shrinkage of polymers is limited. Then the conductive network was destroyed under the action of the thermal residual stresses, the contact of CB particles coated PET microfibrils was partly broke, the distances between different PET microfibrils increase due to the tiny thermal movement of the microfibrils and CB particles, thereby, influences the electrically conductive properties of CPC. But for the sample with HCR180, after long time and high temperature thermal treatment, the aggregation of PET microfibrils is fine, the conductive network is nice. So the motion of PET microfibrils is hard, they would not be easily affected by the thermal residual stress, and the shrinkage of polymers is the key factor, which results in more fine conductivity. Fig. 13 illustrates the microstructure change model for HCR140 (c) and HCR180 (b) samples.

For the HCR140 sample (Fig. 13(c)), because of the short treatment time in the molten matrix, aggregation of conductive fillers is limited, and the distance between the neighboring PET microfibrils is large. The conductive path by the contact of PET microfibrils is poor and easily vulnerable by the thermal residual stresses. Here the thermal residual stresses are the main element affecting the resistivity of the HCR140 sample. Therefore, in the cooling process below 100 °C, the conductive contact between CB coated PET microfibrils is destroyed, leading to the increasing distances between conductive PET microfibrils. By tunneling mechanism, this case will affect the conductive network, thus the resistivity of the CPC.

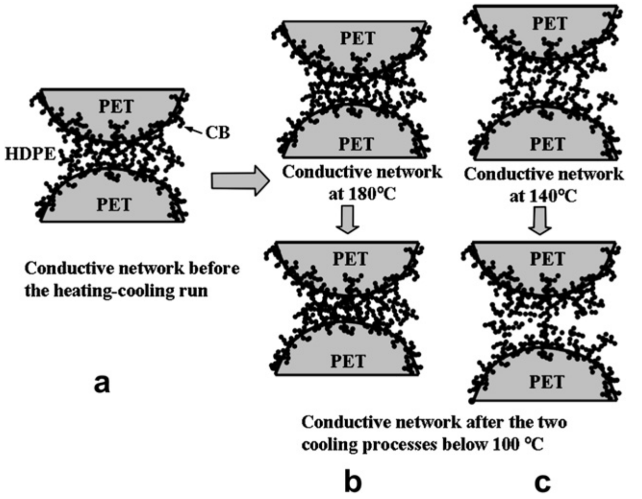

Fig. 13. Illustration of the movement of microfibrils and CB particles with the decreasing temperature below 100 °C. The gray domains are the crosssection of PET microfibrils with CB coating on their surfaces. The black points are carbon black.

Due to the tunneling mechanism proposed by Balberg et al. [41–43], the minute increase of the distances between PET microfibrils and/or between CB particles results in an obvious increase of the resistivity.

$$\sigma_{\mathrm{tun}} \propto \exp\left[-\frac{r-2b}{d}\right] \tag{2}$$

where σ_{tun} is the inter-particle tunneling conductivity, r is the distance between the centers of the particles, b is the radius of the particles and d is the typical tunneling range (or tunneling decay) parameter. As clearly suggested by Eq. (2), every two particles (here assumed spherical) in the system are electrically connected, and their contribution to the conduction of the whole network diminishes as r increases.

Therefore, under the action of the thermal residual stresses, the PET microfibrils motioned gradually, the distances between many CB coated PET microfibrils grew gradually, thus largely dominating the resistivity of the FCMC during cooling below 100 °C. With the increasing distances between PET microfibrils, the distances between CB particles on the PET microfibrils also increased. Considering the tunneling mechanism (as Eq. (2)), the raise of r results in obvious decrease of the conductivity, i.e., the increase of the resistivity. As a result of this, the resistivity of the FCMC increases significantly with decreasing temperature. But for samples with HCR180, the volume shrinkage of polymers is the main factor, which led to more fine conductive contact and a better conductivity.

In the studies by Hirano and Kishimoto [21] and Li et al. [24], different heating or cooling rates can result in obvious difference in resistivity–temperature behaviors. In their

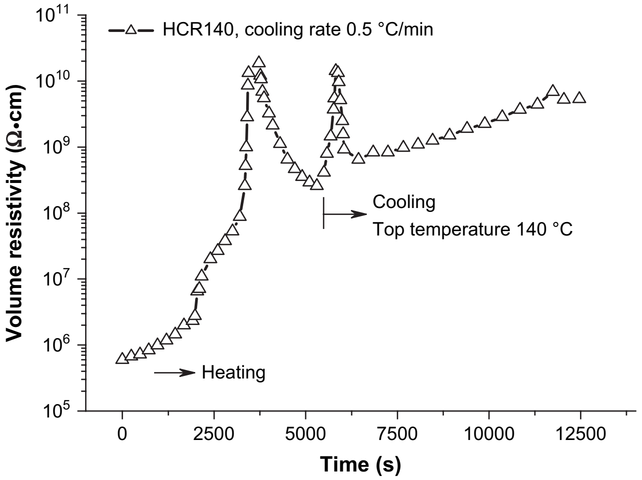

Fig. 14. Resistivity–temperature relationship of the CB filled electrically conductive in situ microfibrillar PET/PE composite in the heating–cooling run with a top test temperature of 140 °C (HCR140). The heating and cooling rates are 2 °C/min and 0.5 °C/min, respectively.

works, a faster heating rate led to a higher PTC intensity [24]. They thought that the heating rate dependence of the anomaly was strongly related to the thermal strain rate of the polymer matrix. A slow rate leads to the relaxation of the polymer matrix and the decay of the stress (expansion stress [21] or internal stress [24]). To confirm the effect of the cooling rate to the thermal residual stresses and this abnormal phenomenon of FCMC, a slower cooling rate was set at 0.5 °C/min for HCR140 sample.

Fig. 14 shows the resistivity–temperature behavior for HCR140 sample at a cooling rate of 0.5 °C/min. The resistivity–temperature behavior during heating is nearly the same as Fig. 5. However, during cooling, the cooling-induced resistivity increase could also be observed. Hence, the increasing tendency of the resistivity becomes flatter than that of the test at a cooling rate of 2 °C/min (see Figs. 5 and 14). A much slower rate is beyond the limit of the test specification of the temperature regulator, so the resistivity–temperature behaviors during cooling with a much slower rate cannot be attainable. Nevertheless, it is believed that if the cooling rate is slow enough, because of the relaxation of the PET and PE, the thermal residual stresses will fade away, and this cooling-induced resistivity increase should disappear.

Apparently, the above model can successfully explain the cooling-induced resistivity increase of FCMC. Furthermore, this phenomenon is also related to the room-temperature resistivity, reproducibility and the crystallization of the FCMC as a PTC material, being of significance to its application. It always makes the room-temperature resistivity rise, and causes poor reproducibility.

In order to study the effect of annealing at 140 °C, the resistivity–temperature behaviors were also tested during cooling after the annealing at 140 °C for two times: 1 h, and 10 h as shown in Fig. 15. After 1 h and 10 h, the increase of the cooling-induced resistivity disappeared because of fading away of the thermal residual stresses, i.e., a similar cooling behavior as for the HCR180 was observed, but a lower relative room-temperature resistivity was obtained for the 10 h annealing. Among the samples with annealing at 140 °C for 1 h and 10 h, and the HCR180, the samples with HCR180 shows the lowest relative room-temperature resistivity, which indicates that the best conductive network is formed for HCR180, and the temperature has stronger availability than the time in HDPE melt in the tests.

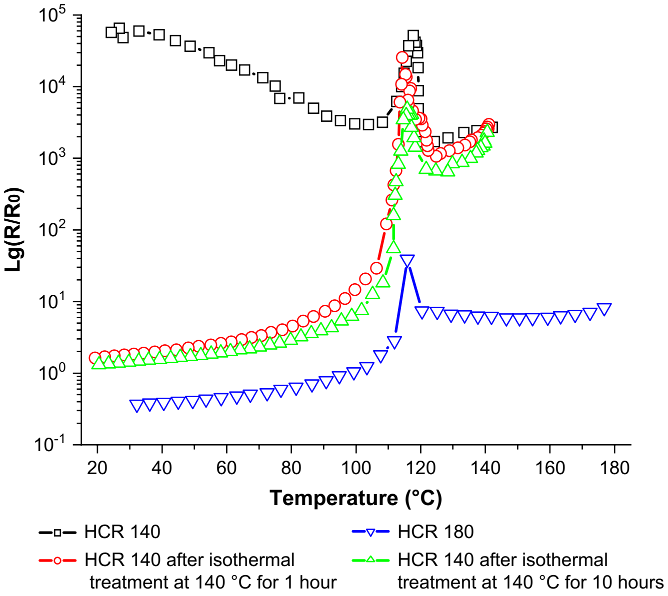

Fig. 15. Resistivity–temperature relationships of the CB filled electrically conductive in situ microfibrillar PET/PE composite in the heating–cooling run with a top test temperature of 140 °C and 180 °C (HCR140, HCR180), and in the heating–cooling run with a top test temperature of 140 °C (HCR140) after 1 h and 10 h isothermal treatment, respectively.

If the common CB/PE composites experiences HCR140, the cooling-induced resistivity increase is yet not observed (Fig. 16). But the room-temperature conductivity of the CPC

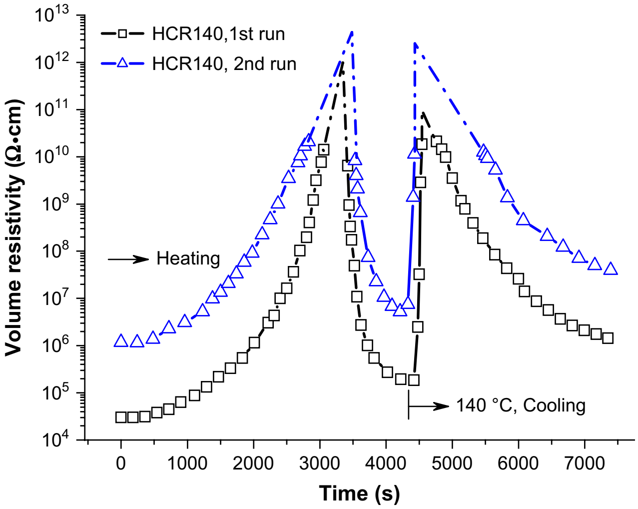

Fig. 16. Resistivity–temperature relationship of CB/PE conductive polymer composite with 8.68 vol% CB with a top test temperature of 140 °C (HCR140) for two heating–cooling runs. The heating and cooling rates are both 2 °C/min. The imaginary line denotes that the resistivity is beyond the test specification of the electrical meter.

also becomes worse than the conductivity before the test. It is known the CB particles will reject from the crystallites and can only reside in the amorphous regions [26]. Hence, though there is no enough time for CB particles to form a fine conductive network in the heating process, the CB particles will reject from the crystallites and accumulate in the amorphous regions in the cooling process. Moreover, with the shrinkage of PE, many conductive paths could also be formed, so the cooling-induced resistivity increase does not occur. However, due to the weak aggregation in the molten PE matrix, the room-temperature resistivity of the sample also increases. As common PTC materials, this change of the room-temperature resistivity is significative for the industrial application of the CB/PE CPC.

5. Conclusions

The CB filled electrically conductive in situ microfibrillar PET/PE composites (FCMC) were successfully prepared using the slit die extrusion–hot stretch–quenching process. In this composite, most CB particles were distributed at the surfaces of PET microfibrils, but there are still some CB particles left in the matrix. A low percolation threshold was obtained (3.8 vol%). The conductive network of the FCMC was formed by the contact of the CB particles coated PET microfibrils.

After 10 h isothermal treatment at 180 °C, the PTC intensity decreased obviously (from 5 to 1.2), interestingly, the NTC effect disappeared. The increasing contact of PET microfibrils as a result of their heat motion in the molten matrix is responsible for this phenomenon. The top test temperatures in heating–cooling runs for FCMC dominated resistivity–temperature behaviors during cooling below 100 °C. When the top test temperature was set at 140 °C, the resistivity of the FCMC increased obviously during cooling below 100 °C, showing cooling-induced resistivity increase. After the first HCR140, the room-temperature resistivity of FCMC was 4 orders of magnitude higher than that of the original samples. The damage of the conductive network by the thermal residual stresses developed at the interfaces between PET microfibrils and PE matrix is the main reason. The room-temperature resistivity of common CB/PE CPC also increased after the HCR140.

The cooling-induced resistivity increase is related to the room-temperature resistivity, reproducibility and the crystallization, so it is significative for the applications of the PTC materials, over-current, self-regulating heaters, etc. Based on the special microstructure that the CB particles were distributed at the surfaces of PET microfibrils and the conductive network constructed by PET microfibrils, the structure of the CPC, especially the distribution of conductive fillers, affects the properties of the PTC materials significantly. The most important result is that the cooling-induced resistivity increase indicates that the work about the cooling process of the PTC materials is sufficiently necessary.

Acknowledgements

The authors gratefully acknowledge the financial support of this work by the Nature Science Foundation of China (Contract Number: 50573049) and Specialized Research Fund for the Doctoral Program of Higher Education (Contract No. 20060610026). Thanks are also given to Mr. Zhu Li from Analytical & Test Center of Sichuan University for his help in the SEM observation.

References

[1] Meyer J. Polym Eng Sci 1974;14:706–16.
[2] Mironi-harpaz I, Nakis M. Polym Eng Sci 2001;41:205–21.
[3] Mironi-harpaz I, Nakis M. J Polym Sci Part B Polym Phys 2001; 39:1415–28.
[4] Xu XB, Li ZM, Dai K, Yang MB. Appl Phys Lett 2006;89:032105.
[5] Wu TM, Cheng JC, Yan MC. Polymer 2003;44:2553–62.
[6] Feng JY, Chan CM. Polymer 2000;41:4559–65.
[7] Hindermann-Bischoff M, Ehrburger-Dolle F. Carbon 2001;39:375–82.
[8] Tang H, Chen XG, Luo YX. Eur Polym J 1997;33:1383–6.
[9] Yui HS, Wu GZ, Sano HN, Sumita M, Kino K. Polymer 2007;47: 3599–608.
[10] Szleifer I, Yerushalmi-Rozen R. Polymer 2005;46:7803–18.
[11] He XJ, Du JH, Ying Z, Cheng HM. Appl Phys Lett 2005;86:062112.
[12] Chen QY, Bin YZ, Matsuo Masaru. Macromolecules 2006;39: 6528–36.
[13] Heaney MB. Appl Phys Lett 1996;69:2602–4.
[14] Azulay D, Eylon M, Eshkenazi O, Toker D, Balberg M, Shimoni N, et al. Phys Rev Lett 2003;90:236601.
[15] Duggal AR, Levinson LM. Appl Phys Lett 1997;71:1939–41.
[16] Song YH, Pan Y, Zheng Q, Yi XS. J Polym Sci Part B Polym Phys 2000;38:1756–63.
[17] Meyer J. Polym Eng Sci 1973;13:462–86.
[18] Ohe K, Naito Y. Jpn J Appl Phys 1971;10:99–108.
[19] Voet A. Rubber Chem Technol 1981;54:42–50.
[20] Feng JY, Chan CM. Polymer 2000;41:7279–82.
[21] Hirano S, Kishimoto. Appl Phys Lett 1998;73:3742–4.
[22] Luo YL, Wang GC, Zhang BY, Zhang ZP. Eur Polym J 1998;34: 1221–7.
[23] Yi SY, Wu GZ, Pan Y. Polym Int 1997;44:117–24.
[24] Li RQ, Dou DY, Miao JL, Wang WF, Yao SD, Zeng HM. J Appl Polym Sci 2002;86:2217–21.
[25] Di WH, Zhang G, Xu JQ, Peng Y, Wang XJ, Xie ZY. J Polym Sci Part B Polym Phys 2003;41:3094–101.
[26] Babinec SJ, Mussell RD, Lundgard RL, Cieslinski R. Adv Mater 2000;12:1823–34.
[27] Li ZM, Xu XB, Lu A, Shen KZ, Huang R, Yang MB. Carbon 2004;42:428–32.
[28] Xu XB, Li ZM, Yang MB, Jiang S, Huang R. Carbon 2005;43:1479–87.
[29] Xu XB, Li ZM, Yu RZ, Lu A, Yang MB, Huang R. Macromol Mater Eng 2004;289:568–75.
[30] Dai K, Xu XB, Li ZM. Polymer 2007;48:849–59.
[31] Zheng Q, Song YH, Wu G, Song XB. J Polym Sci Part B Polym Phys 2003;41:983–92.
[32] Song YH, Zheng Q. J Appl Polym Sci 2007;105:710–7.
[33] Xi Y, Ishikawa H, Bin YZ, Matsuo M. Carbon 2004;42:1699–706.
[34] Bueche F. J Appl Phys 1973;44:532–3.
[35] Chan CM, Cheng CL, Yuen MMF. Polym Eng Sci 1997;37:1127–36.
[36] Tang H, Piao JH, Chen XF, Lou YZ, Li SH. J Appl Polym Sci 1993;48:1795–800.
[37] Yi XS, Zhang JF, Zheng Q, Pan Y. J Appl Polym Sci 2000;77:494–9.
[38] Wu GZ, Asai S, Sumita M. Macromolecules 1999;32:3534–6.
[39] Boyce ME, Argon AS, Parks MD. Polymer 1987;28:1680–94.
[40] Sue HJ, Huang J, Yee AF. Polymer 1992;33:4868–71.
[41] Balberg I, Azulay D, Toker D, Millo O. Int J Mod Phys B 2004; 18:2091–121.
[42] Grimaldi C, Balberg I. Phys Rev Lett 2006;96:066602.
[43] Rubin Z, Sunshine SA, Heaney MB, Bloom I, Balberg I. Phys Rev B 1999;59:12196–9.